

SD-GAN: Semantic Decomposition for Face Image Synthesis with Discrete Attribute

Kangneng Zhou
g20208857@xs.ustb.edu.cn
Department of Computer Science, University of
Science and Technology Beijing, China

Xiaobin Zhu*
zhuxiaobin@ustb.edu.cn
Department of Computer Science, University of
Science and Technology Beijing, China

Daiheng Gao
daiheng.gdh@alibaba-inc.com
DAMO Academy, Alibaba Group, China

Kai Lee
b20200344@xs.ustb.edu.cn
Department of Computer Science, University of
Science and Technology Beijing, China

Xinjie Li
abcdvzz@hotmail.com
Department of Computer Science, University of
Science and Technology Beijing, China

Xu-Cheng Yin
xuchengyin@ustb.edu.cn
Department of Computer Science, University of
Science and Technology Beijing, China
USTB-EEasyTech Joint Lab of Artificial
Intelligence, University of Science and
Technology Beijing, China

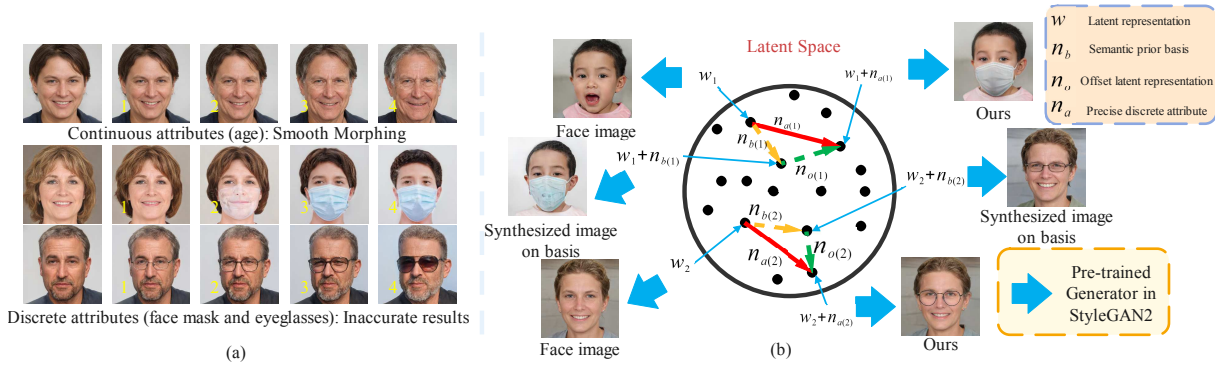


Figure 1: Motivation and solution of our method. (a): Morphing results of continuous attributes (age) and discrete attributes (face mask and eyeglasses) via InterfaceGAN [41] with different length. Discrete attributes synthesis is inaccurate. **(b):** Schematic diagram of manipulating face representation in latent space. The yellow arrows indicate semantic prior basis n_b for synthesizing images. The green arrows indicate the offset latent representation n_o of facial attributes. The red arrows indicate the precise semantic representation n_a in our method. w is the face latent representation in the latent space of pre-trained StyleGAN2. Notice that each face representation has its unique discrete attribute code. Our method has the state-of-the-art performance.

ABSTRACT

Manipulating latent code in generative adversarial networks (GANs) for facial image synthesis mainly focuses on continuous attribute synthesis (e.g., age, pose and emotion), while discrete attribute synthesis (like face mask and eyeglasses) receives less attention. Directly applying existing works to facial discrete attributes may cause inaccurate results. In this work, we propose an innovative framework to tackle challenging facial discrete attribute synthesis via semantic decomposing, dubbed SD-GAN. To be concrete, we explicitly decompose the discrete attribute representation into two components, i.e. the semantic prior basis and offset latent representation. The semantic prior basis shows an initializing direction for manipulating face representation in the latent space. The offset latent presentation obtained by 3D-aware semantic fusion network is proposed to adjust prior basis. In addition, the fusion network integrates 3D embedding for better identity preservation and discrete

attribute synthesis. The combination of prior basis and offset latent representation enable our method to synthesize photo-realistic face images with discrete attributes. Notably, we construct a large and valuable dataset MEGN (Face Mask and Eyeglasses images crawled from Google and Naver) for completing the lack of discrete attributes in the existing dataset. Extensive qualitative and quantitative experiments demonstrate the state-of-the-art performance of our method. Our code is available at an anonymous website: <https://github.com/MontaEllis/SD-GAN>.

CCS CONCEPTS

• Computing methodologies → Image processing.

KEYWORDS

Decomposing Face Attribute Representation; Face Discrete Attribute Synthesis; 3D-aware; GAN

*Corresponding author.

1 INTRODUCTION

Image synthesis has various applications, such as interactive graphics editing and image translation. With the rapid development of deep learning, image synthesis has achieved promising performance and received ever-increasing interest. Among different categories of natural images, it is very challenging to synthesize discrete attributes of face images (e.g., face mask and eyeglasses) mainly due to the complicated structure of face images and the complex geometric relationships between face images and discrete attributes.

Image-to-image translation methods on face image synthesis try to learn mapping relationships among different image domains [21, 47, 64]. Generally, these methods achieve synthesis realism from appearance space while neglecting the critical geometry space. Some other techniques adopt image composition strategies to fuse foreground image (e.g., face mask) with background image (face image) [28, 54]. SF-GAN [54] combines a geometry synthesizer with an appearance synthesizer to achieve synthesis realism. Although these methods can keep other face attributes intact, they often suffer from the different distributions of two image domains, resulting in non coherent fusing edges.

Recently, learning facial semantics via manipulating latent code in the latent space has achieved great success in high-fidelity face image synthesis [16, 41, 43]. GANSpace [16] adopts PCA to find facial semantic representation in the latent space of the GAN model. StyleSpace [50] utilizes style channels to control a highly disentangled visual attribute. These methods usually modify a latent code and enable semantic-level editing for generated images. They can synthesize faces with fine visual details, however, most of them mainly focus on continuous attributes (e.g., age, pose and emotion). When applying these methods to tackle facial discrete attribute synthesis, the results are always inaccurate. As shown in Fig. 1, the attribute representation in yellow arrows facilitates poor results which drift the accurate ones in red arrows. In addition, according to [46] the manifold corresponding to 2D images in the latent space do not allow to control accurately 3D shapes. The 3D-aware GANs have abundant 3D information but there are few works introduce them to facilitate 2D face image synthesis.

To address the above-mentioned problems, we propose an innovative framework (named SD-GAN) to decompose the latent code of facial and discrete attributes in the latent space of GANs. From our key observations (as shown in Fig. 1(a)), face image synthesis networks [41] fail in regressing accurate discrete attributes which are orthogonal to other facial attributes. For example, while manipulating face mask attribute on the second row of Fig. 1(a), the age and hair of the face changed as well. Hence, we decompose the semantic discrete attribute into prior basis and offset latent representation. As shown in Fig. 1, the optimal face images always correspond to different lengths of basis. So a novel search algorithm is also proposed for the optimal length of the basis. In this way, the semantic prior basis shows an initializing direction for manipulating face representation and makes the network focus on learning the following offset latent representation instead of losing its way in the large possible latent space.

In addition, highly motivated by the 3D controlling abilities of 3D-aware GAN [4, 11, 12, 31, 49, 62], we propose a novel 3D-aware semantic fusion network to generate offset latent representation of

discrete attributes for adjusting prior basis and performing better authentic. In this way, we introduce 3D embedding into 2D manifolds to help the network perform better in identity preservation and discrete attribute synthesis. The offset latent representation and semantic prior basis will be combined to facilitate the original latent code for generating the final synthesized image. As shown in Fig. 1, with the help of W prior basis, the network easily converges to precise latent representation. Our method has the advantages of both face attribute intacting and visual details. Notably, we construct a dataset MEGN (Face Mask and EyeGlasses images crawled from Google and Naver). According to the experimental results in Sec. 4, our MEGN greatly benefits the task of synthesizing images with discrete attributes. In summary, our contributions are:

- We propose an innovative framework (named SD-GAN), decomposing semantic discrete attribute representation in the latent space of GANs into semantic prior basis and offset latent representation. Our method achieves state-of-the-art performance both qualitatively and quantitatively.
- We adopt the normal vector of the hyperplane created by a SVM classifier as the semantic prior basis and a novel optimal length of basis search algorithm is proposed therein. The semantic prior basis shows an initializing direction for manipulating face representation in the latent space. Also, a novel 3D-aware semantic fusion network is proposed to generate offset latent representation. 3D information is integrated in the network for achieving better authenticity.
- We propose a valuable dataset MEGN for complementing existing datasets that are lacking in discrete attributes, for the task of face image synthesis.

2 RELATED WORK

2.1 Image Synthesis via GAN

Image synthesis aims to fuse with other objects for generating realistic images while the remaining attributes in the un-covered part of the image are unchanged. Image-to-image translation methods try to learn optimal mapping relationships between different image domains for image synthesis. A lot of works adopt conditional GAN [21], dual learning [21], multi-domain transformation [64], separated latent space swapping [9] and other novel methods [6, 22, 30] to synthesize general face attributes. Overall, the existing image-to-image translation methods often achieve synthesis realism from appearance space while neglecting the geometry space. Image-Composition based methods try to blend foreground images with a background image into a target image. ST-GAN [28] adopts geometric warping parameter space to synthesize images with geometric realism, but it neglects the appearance of realism. SF-GAN [54] adopts a spatial fusion strategy to synthesize images for both appearance realism and geometric realism.

Generally, image-composition based methods tend to suffer from different distributions of two image domains, resulting in incoherent fusing edges. Our method works in a semantic latent space rather than the methods mentioned above.

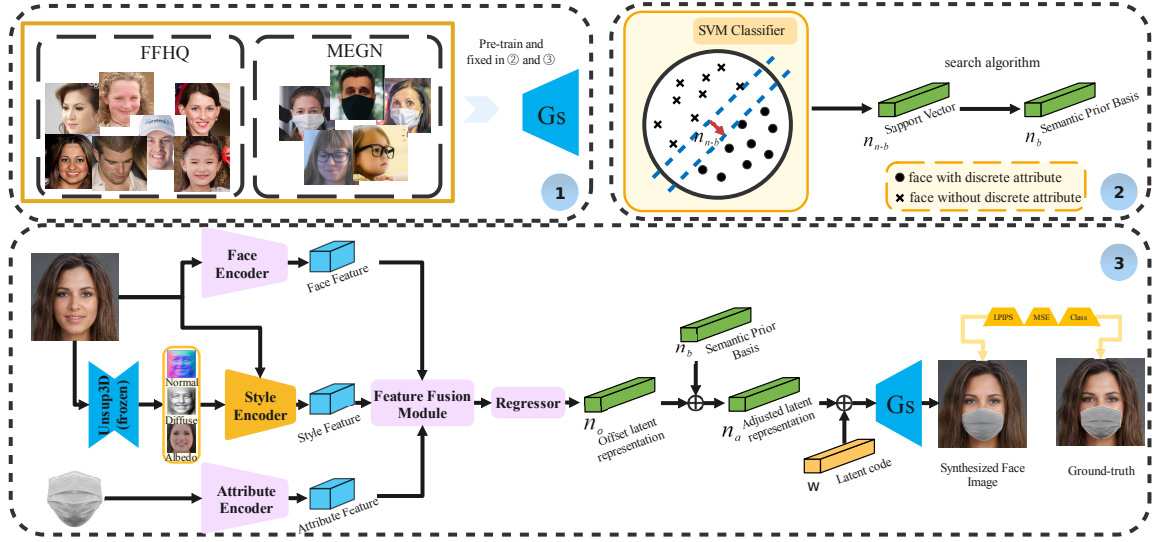


Figure 2: Framework of our method. (1): Diagram of StyleGAN2 pre-training. (2): Flowchart of generating semantic prior basis. (3): 3D-aware Fusion Network for offset latent representation. Our method decomposes facial attribute into semantic prior basis and offset latent representation, facilitating face synthesis with discrete attribute. The offset latent representation obtained by 3D-aware fusion network balances a better authenticity between face images and discrete attribute.

2.2 Latent Semantic Manipulating

Recently, image synthesis methods via manipulating the latent representation have achieved promising performance and attracted great attention. Chen *et al.* [7] separates an input noise vector into an incompressible part and a latent code; hence it can concentrate on exploring semantic information underlying latent representation for generating synthesis images. StyleGAN [24] is proposed to demonstrate the potential power of decoupling attributes in latent space to highlight the particular semantic attribute.

Shen *et al.* [41] hypothesize that the latent representations of two face images can be separated by a normal vector in latent space, which can be utilized to implement controllable face image synthesis. Härkönen *et al.* [16] adopt PCA to find the principle face attribute representation in the latent space of GAN model. Shen and Zhou [43] propose an unsupervised method to find semantic representations for tackling some undefinable attributes, e.g., eye size and painting style. Tewari *et al.* [46] proposes a method to embed a parametric face model into the network and implement pose, illumination manipulation. StyleCLIP [36] conducts image manipulation via a text-based interface for integrating the advantages of CLIP [38] and StyleGAN. Hu *et al.* [20] investigates reference and label attribute editing through a pre-trained latent classifier. Overall, the existing GAN-based methods mainly focus on continuous attributes and often fail to hold discrete ones. Our method aims to synthesize faces with discrete attributes correctly.

2.3 3D-aware GAN

The works in GANs has promising performance, while the series of StyleGANs [23–25] lack the ability to hold 3D controls and have difficulty to achieve complex editing. Recent works leverage Neural

Radiance Field (NeRF [29]) to construct implicit fields to represent 3D scenes. The following works [5, 12, 31, 63] adopt periodic implicit GAN, progressively upsampling, Implicit Neural Representation [8] and Signed Distance Function (SDF) [34] to synthesize 3D-aware data. Head-NeRF [18] is proposed to take 3DMM as prior to construct a face field. Other methods focus on wild images and reconstruct 3D faces in supervised [15, 69] or unsupervised ways [33, 49]. Our method embeds 3D information obtained by 3D-aware Unsup3d [49] into semantic fusion network to synthesize images with authenticity.

3 OUR METHOD

3.1 Overview

The framework of our method is illustrated in Fig. 2. In step one of Fig. 2, we will first pre-train the generator of StyleGAN2 G_s on FFHQ and our proposed MEGN. Then our generator will be fixed after pre-training. To decompose semantic attribute representation, we explore a semantic prior basis via an SVM classifier in the latent space in step two. 3D-aware semantic fusion network is proposed in step three, feature of face image and discrete attribute will be extracted by two individual encoders. The face image, and its corresponding 3D information extracted by Unsup3D [49], will be combined to extract the feature by style encoder. The three features (face feature, attribute feature and style feature) will be used to learn offset latent representation by fusion module. The offset latent representation and semantic prior basis will be combined into an adjusted latent representation for promoting the latent representation of the original face image. The synthesized face image will be generated by the pre-trained generator G_s .

3.2 Semantic Prior Basis

The synthesis network of StyleGAN2 [25] in the series of StyleGAN [23–25] can be explained as a function G_s that maps a latent code $w \in \mathbb{R}^{512}$ to a realistic face image $I = G_s(w)$. A hyperplane in the latent space serves as a decision boundary to separate the face attributes. Learning the hyperplane mainly consists of three steps. First, we sample 500k latent codes $w \in \mathbb{R}^{512}$ and generate the corresponding face images $I_s = G_s(w)$ using a pre-trained generator of StyleGAN2. Then, an attribute prediction model F_{pred} will be adopted to compute a confidence score for the attribute of each image $conf = F_{pred}(I_s)$. We get the training set $\{w, conf\}$ and sort the corresponding scores and choose samples with extremely high scores as positive and extremely low ones as negative.

Finally, an SVM classifier will be trained among the dataset above and resulting in a decision boundary in the latent space. The normal vector of the decision boundary is normalized as semantic prior basis $n_{n-b} \in \mathbb{R}^{512}$ in the latent space of pre-trained StyleGAN2, as shown in Fig. 2 (2).

However, the semantic prior basis obtained by the SVM classifier cannot distinguish different facial attributes (with or without discrete attribute) in the non-compact and unsmooth latent space of GAN. As shown in Fig. 1, the optimal images correspond to different lengths of prior basis. The face in the second row with length of 3 is the optimal while the face in the third row is optimal with weight of 2. In order to promote the initialized guide capability of prior basis, we adopt a novel search algorithm to compute an optimal length η for the semantic prior basis of each face image. Specifically, we search for an optimal face image with discrete attributes while maintaining the identity as best as possible. We compute the length η according to a formula that consists of three parts and formulated as below:

$$\begin{aligned} Score = & F_{det}(G_s(w + \eta * n_{n-b})) \\ & + \lambda \times \|M \odot (G_s(w + \eta * n_{n-b}) - G_s(w))\|_2^2 \\ & - \lambda \times \|\bar{M} \odot (G_s(w + \eta * n_{n-b}) - G_s(w))\|_2^2, \end{aligned} \quad (1)$$

where F_{det} represents a discrete attribute detector which is trained by YOLO [39] whose confidence scores are used here, G_s represents the synthesis network of generator in StyleGAN2, w represents the latent code of face image ($w \in \mathbb{R}^{512}$), M represents the binary mask of face which can be obtained by the method in Sec. 4.2.2, and \bar{M} represents the area which does not belong to binary face mask, λ is used to balance loss terms and is set to 10 here.

The first part in Eq. 1 aims to force the network to learn the discrete attribute. The discrete attributes are harder than continuous ones to be disentangled among other attributes, so this part of loss is significant. The second part aims to morph the area of simulated discrete mask dramatically, which can improve the possibilities of correct manipulation and prevent the network from falling into local optima that do not update. The third part aim to maintain identity information while manipulating discrete attributes, which is significant for accurate discrete attribute manipulating.

We have a series of weights $\{\eta_1, \eta_2, \dots\}$ increasing linearly from 0 to 10 with step of 0.2 and selecting η_m to maximize $Score$. The η_m is regard as the optimal length and compute semantic prior basis:

$$n_b = \eta_m * n_{n-b} \quad (2)$$

3.3 3D-aware Semantic Fusion Network

Existing GAN-based methods generally adopt linear strategies to directly regress semantic representation [41]. These methods sometimes even fail in disentangling continuous attributes (e.g hair, smile, age), still less discrete attributes. Distinguished from existing methods, in our work, we aim to explicitly decompose the discrete attribute representation so that the network would focus on offset latent representation with the benefit of initializing direction of prior basis. The detailed structure of the 3D-aware semantic fusion network is illustrated in Fig. 2 (3). Given a face image I_f generated by StyleGAN2 [25] and a discrete attribute image I_m , the 3D-aware semantic fusion network learns a mapping function f_m for correlating their latent semantic representations as:

$$n_o = f_m(I_f, I_m), \quad (3)$$

where n_o is the offset latent representation obtained by our semantic fusion network. It is worth noticing that $n_o \in \mathbb{R}^{14 \times 512}$ ($W+$ space which is more expressive than W space). The $W+$ is an extended latent space which consolidates 14 different $w \in \mathbb{R}^{512}$ code from W space. The face latent codes w here are sampled from the mapping network in StyleGAN2, so $w \in \mathbb{R}^{512}$. The w can translate to $W+$ space via broadcasting. The Ground-truth of the training process can be found in Sec. 4.2.2.

Here, we dissect the design of each sub-module (illustrated by pink boxes and yellow box in Fig. 2). The face encoder is designed to learn object-specific features, which serves to preserve identity-information for the final results. Inspired by works in face recognition, the weights in face encoder are initialized by ArcFace [10] for better extracting unique face features at the beginning of training. For attribute encoder, we adopt the first four residual blocks of ResNet-18 [17] to extract the feature.

The fixed Unsup3d [49] is applied to get normal map, diffuse map and albedo. The normal map contains fine detailed shape of the face, while diffuse map and albedo represent the texture of the face. Our style encoder (the yellow box in Fig. 2) consists of multi-layer convolutions to reflect sufficient 3D expression features from the concatenation of face normal map, diffuse map, and albedo images. In this way, the style encoder is expressive for 3D shape to estimate the position of discrete attributes and has adequate 3D information which can reconstruct the face to enhance the ability of identity preservation. With object-specific face feature, discrete attribute feature and adequate 3D feature, we propose a fusion module to fuse features and make them fully expressive for unique precise discrete attribute features. Inspired by SEAN [66], our feature fusion module adopts weighted learning with coefficients to fuse the extracted features. The details of network architecture of style encoder and fusion module can be found in Appendix.

Our regressor aims to map the fused feature to offset latent representation in the $W+$ space mentioned above. Our regressor consists of sparse-connected layers [40] for mapping operation, which avoids the issue of redundant parameters in fully-connected layers. The structure not only has fewer parameters, but also has stronger performance capabilities.

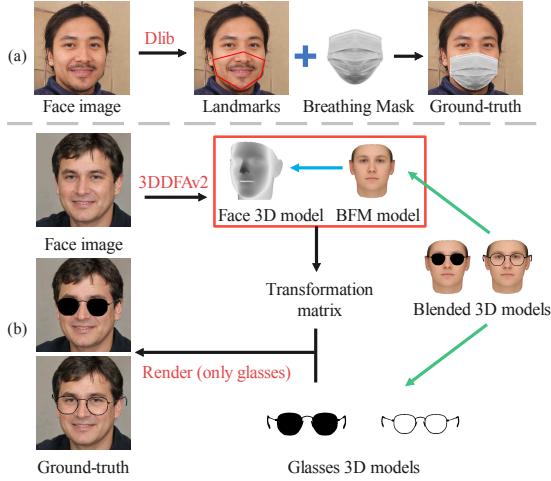


Figure 3: Pipeline of generated synthetic dataset. (a): Ground-truth of face image generation with face mask. (b): Ground-truth of face image generation with different eye glasses.

So far, we get the adjusted latent code n_a through the addition of offset and n_b :

$$n_a = n_o + n_b \quad (4)$$

With the adjusted latent representation n_a , we can modulate the latent representation w for generating a synthesized image with discrete attributes while retaining other attributes intact. Mathematically, it can be formulated as:

$$I_{pred} = G_s(w + n_a), \quad (5)$$

where I_{pred} represents the synthesized face image with discrete attribute.

3.4 Optimization

We adopt MSE (Mean Squared Error) to evaluate the content loss of synthesized image, which can be formulated as:

$$L_{mse} = \|I_{pred} - I_{gt}\|_2^2, \quad (6)$$

where I_{gt} represents Ground-truth in Sec. 4.2.2. We adopt LPIPS [58] loss to evaluate feature-level inconsistency, which can be formulated as:

$$L_f = \Phi(I_{pred}, I_{gt}), \quad (7)$$

where Φ represents LPIPS [58] loss.

In order to explicitly guide the network to converge in the direction of face image with discrete attribute, we adopt a class loss which can be formulated as:

$$L_c = 1 - F_{det}(I_{pred}), \quad (8)$$

where F_{det} represents the classification network which is the same as Eq. 1 of the discrete attribute.

Finally, the total loss for our method is:

$$L_{all} = L_{mse} + \lambda_1 L_f + \lambda_2 L_c, \quad (9)$$

where λ_1 and λ_2 are empirically defined parameters.

4 EXPERIMENTS

4.1 Implementation Details

The backbone of our face image encoder is a pre-trained ArcFace [10]. In our network training, Adam [27] optimizer is applied to train our model with 30 epochs. The batch size is set to 10. The initial learning rate is 0.01 and multiplied by 0.8 after each 5 epoch. The parameters in the generator are fixed during the whole training process. We evaluate our method on 1,000 images randomly sampled from the pre-trained StyleGAN2. All experiments are performed on a single GPU (RTX-3090), and PyTorch 1.6.0.

4.2 Dataset setting

4.2.1 Our MEGN for training generator. It is worth noting that the generator in StyleGAN2 [25] trained by FFHQ cannot successfully generate images with face mask and eyeglasses. Existing face image datasets with discrete attribute are mainly designed for the task of face detection [48], in which the face targets are generally small and fuzzy. Hence, they are not consistent with the distribution of FFHQ. Although there are some synthetic fake datasets [3], they are not realistic in subjectivity for network training.

To obtain high-resolution images close to the distribution of FFHQ, we manually construct our MEGN (Face Mask and Eye-Glasses images crawled from Google and Naver), which includes 5,000 face images with the attributes of wearing a face mask and eyeglasses (resolution 256×256). All data in this dataset are carefully crawled from Google and Naver, aligned by Dlib [26]. Then, we manually remove the inaccurate and blurred images.

We pre-train the generator G_s StyleGAN2 on a mixed FFHQ and MEGN dataset, enabling the generator to generate informative images with discrete attributes. To the best of our knowledge, our MEGN is the first realistic, high-definition dataset of face images with discrete attributes, especially face mask. Subsequent experiments (as shown in Sec. 4) have proved that the complement of MEGN is quite useful for the representation and decoupling of discrete attributes in the latent space.

4.2.2 Synthetic dataset for training 3D-aware Fusion Network. Due to the lack of 3D models, we adopt MaskTheFace [1] to synthesize the face mask image. Specifically, face mask is applied to the face with landmarks detected by Dlib [26]. The procedure of synthetic generation is depicted in Fig. 3 (a). In glasses image synthesis, it is difficult to precisely locate the feet of glasses due to the ambiguity of depth and self-occlusion, resulting in an unrealistic image. Highly motivated by the works in [13, 14, 19, 44, 55–57, 59–61, 67, 68], we also adopt 3DDFAv2 [15] to obtain 3D face representation [2] of face image and further find the transformation matrix between BFM [37] and ours. The transformation matrix will be applied to glasses 3D models (pre-registered to BFM). Finally, we render the glasses on top of the current face in Fig. 3 (b). Although we adopt synthetic images as Ground-truth, extensive experiments reveal that our images exceed Ground-truth in terms of many metrics.

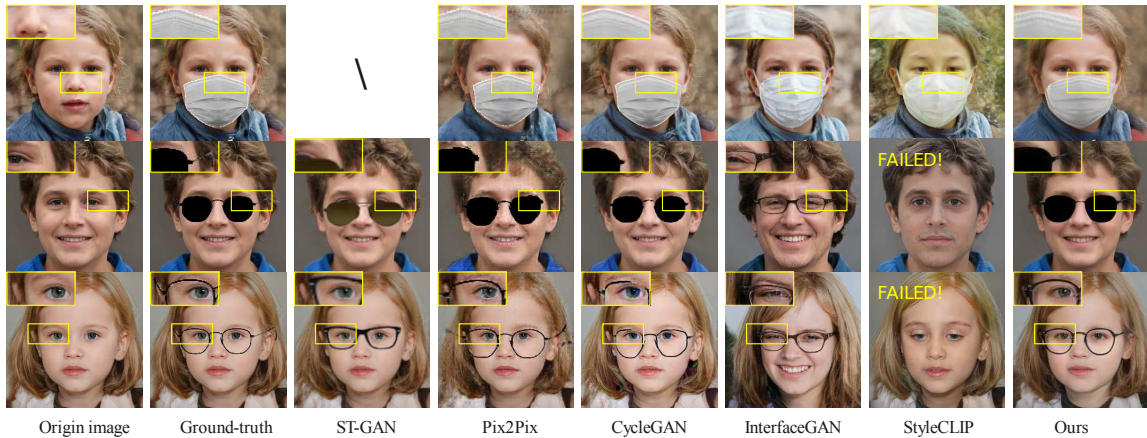


Figure 4: Representative visual results of different methods. Our method outperforms other methods on visual quality.

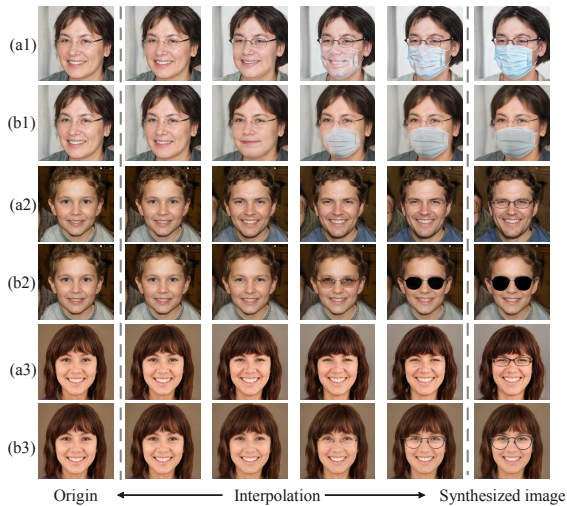


Figure 5: Representative visual results generated by interpolation on latent space of GAN models. (a1-a3): InterfaceGAN, (b1-b3): Our method. Our method outperforms InterfaceGAN in terms of the fluidity and identity preservation.

Extensive experiments have proven our method is generalisable, and for other discrete attributes, the network can achieve more realistic effect by simply simulating Ground-truth as shown in Fig. 3.

4.3 Qualitative Experiments

4.3.1 Synthesis Face Image with Discrete Attributes. For the task of face image synthesis, it is important to generate pleasing visual details (such as coherent edges and complete structure) while keeping other attributes unchanged. The qualitative results are shown in Fig. 4. ST-GAN [28] locates the glasses in the wrong place, which results in an unrealistic appearance. Pix2Pix [21] generates noise artifacts while synthesizing. CycleGAN [64] generates synthesized

images with incoherent edges and incomplete masks. InterfaceGAN [41] is capable of synthesizing realistic face images with discrete attributes but fails to retain other face attributes. StyleCLIP [36] tends to generate inaccurate images. Apparently, our method keeps other face attributes intact as in composition-based methods (Ground-truth, ST-GAN [28]) and image-to-image based methods (Pix2Pix [21], CycleGAN [64]), and synthesizes face images with visual details as in semantic-based methods [41]. Ground-truth suffers from obvious aliasing and has unsmooth edges. Overall, our method outperforms other methods on visual quality especially anti-aliasing and achieves state-of-the-art results.

4.3.2 Image Interpolation. To comprehensively analyze the semantic property, we adopt face image interpolation, which explores the semantic information in face synthesis. According to [65], a suitable synthesis should change the face mask gradually while keeping other attributes unchanged. As shown in Fig. 5, some representative examples of InterfaceGAN [41] implement face synthesis with face mask while suffering from obvious changes in light attribute ((a_1)), age attribute ((a_2)), and shapes of eyes ((a_3)). We find that the image interpolation in our method is reasonable in semantics and does not change the attributes which should be retained compared to InterfaceGAN. For example, our method does not distort the structure of the face or change other attributes of the face. In contrast, both structure distortion and attributes drift of the face occur in the synthesis of InterfaceGAN [41]. StyleCLIP [37] is quite hard to modify images with discrete attribute correctly, so it is not listed in this experiment. Apparently, our method achieves remarkable performance in the image interpolation task.

4.4 Quantitative Experiments

4.4.1 Synthesis Performance Evaluating with Re-score. Here, we adopt Re-score [42, 51] to evaluate the ability to retain attributes via predicting the confidence of face attributes fidelity before and after face synthesis. For a fair comparison, we directly borrow the trained prediction models from the official repository in IALS [53]. Besides, due to the large coverage proportion of face mask, some

Table 1: Experimental results on retaining face attributes in synthesizing. Re-score is adopted to evaluate the effect of retaining face attributes. The best Re-score is highlighted in bold. FM denotes face mask, SG denotes sun glasses, and FG denotes frame glasses. The best results are highlighted in red, and the second-best results are highlighted in blue.

Methods	Male (↓)			Young (↓)			Pose (↓)			Eyeglasses		
	FM	SG	FG	FM	SG	FG	FM	SG	FG	FM (↓)	SG (↑)	FG (↑)
Ground-truth	0.024	0.094	0.056	0.055	0.131	0.060	0.035	0.002	0.014	0.364	0.992	0.987
ST-GAN [28]	-	0.102	0.174	-	0.102	0.210	-	0.022	0.013	-	0.986	0.959
Pix2Pix [21]	0.052	0.180	0.149	0.188	0.118	0.101	0.030	0.014	0.006	0.603	0.992	0.987
CycleGAN [64]	0.028	0.091	0.060	0.032	0.091	0.075	0.029	0.007	0.015	0.395	0.992	0.987
InterfaceGAN [41]	0.116	0.163	0.151	0.106	0.352	0.356	0.043	0.016	0.016	0.367	0.958	0.985
Ours	0.016	0.071	0.127	0.094	0.014	0.026	0.019	0.000	0.012	0.191	0.993	0.988

Table 2: User study results for face image synthesis on face mask, sun glasses, and frame glasses. Original feature retention (ORF), mask synthesis comfort (MSC), and overall quality of synthesis (OQS) are three metrics for evaluation.

Methods	Face Mask			Sun Glasses			Frame Glasses		
	ORF (↑)	MSC (↑)	OQS (↑)	ORF (↑)	MSC (↑)	OQS (↑)	ORF (↑)	MSC (↑)	OQS (↑)
Ground-truth	4.092	2.762	3.062	3.977	2.985	3.308	4.031	2.869	3.254
ST-GAN [28]	/	/	/	3.569	2.369	2.554	3.715	2.869	3.038
Pix2Pix [21]	3.277	2.685	2.838	2.712	2.185	2.269	3.223	2.438	2.685
CycleGAN [64]	3.923	2.838	3.162	3.754	2.846	3.100	3.915	2.762	3.192
InterfaceGAN [41]	2.069	3.985	3.115	3.408	4.285	3.823	3.169	4.277	3.877
StyleCLIP [36]	3.078	1.674	2.154	3.215	1.349	2.679	3.219	1.561	3.476
Ours	3.992	3.715	3.854	4.077	3.831	3.947	4.077	4.131	4.138

concealed attributes, such as smiles, are not considered in our experiments. The detailed results are listed in Tab. 1 and we can observe that our method outperforms other methods on most attributes according to the Re-score metric. Our method outperforms InterfaceGAN [41] on the young attribute in frame glasses synthesis by 0.330 in terms of Re-score. Notably, our method outperforms Pix2Pix [21] on the eyeglasses attribute and young attribute in face mask synthesis by 0.412 and 0.094 in terms of Re-score, respectively. Generally speaking, image composition based methods (Ground-truth, ST-GAN [28]) and image-to-image based methods (Pix2Pix [21], CycleGAN [64]) should achieve optimal results on Re-score because they are directly affixed with a discrete attribute or will learn a fine-grained pixel-level mapping relationship. Apparently, our method is comparable with image composition-based and image-to-image translation methods and even outperforms them in some attributes. Although InterfaceGAN [41] achieves promising Re-scores, it greatly changes other attributes, as shown in Fig. 4. StyleCLIP [36] edits incorrect images and the resulting images are almost identical to the original, so it is not listed in the table. Overall, our method achieves promising results in terms of Re-score.

4.4.2 User Study. User study is a human evaluation metric for verifying the quality of synthesized images [52]. To test the quality of generated images comprehensively, we adopt three testing metrics: original feature retention (ORF) for evaluating identity preservation ability while manipulating, mask synthesis comfort (MSC) for evaluating the performance of discrete attribute manipulating, and overall quality of synthesis (OQS) for evaluating the authenticity of global face manipulating. The scores of the above three metrics all

range from 1 to 5. We invited 200 volunteers, and each volunteer was randomly given five sets of images randomly selected from 1,000 groups. Each set includes eight images, i.e., original image, Ground-truth, ST-GAN [28], Pix2Pix [21], CycleGAN [64], InterfaceGAN [41], StyleCLIP [36] and Ours. Every volunteer has the duty to score each set of images separately by three metrics.

The detailed results are listed in Tab. 2. From Tab. 2, we can observe that the image composition-based methods and image-to-image based methods have good ORF but unpromising MSC on discrete masks. InterfaceGAN [41] achieves the best MSC but poor ORF. Although the performance of our method on MSC is not the best, it is very close to InterfaceGAN [41]. About ORF, our method under-performs Ground-truth only 0.1 in face mask. But our method apparently outperforms other methods on ORF in sun glasses and frame glasses synthesis. On OQS, our method outperforms InterfaceGAN [41] by 0.739, 0.124, and 0.261 on face mask, sun glasses, and frame glasses, respectively. Apparently, our method achieves state-of-the-art performance against other methods.

4.5 Ablation Study

To verify the effectiveness of our semantic prior basis and 3D-aware fusion network, we conduct two ablation experiments both qualitatively and quantitatively, as shown in Fig. 6 and Tab. 3.

Comparing the results without semantic prior basis and without 3D information, we observe that synthesized images generated via semantic prior basis are more visually realistic than the results without semantic prior basis (denoted by "Ours (w/o basis)") and the results without 3D information (denoted by "Ours (w/o 3d)"). The results generated via semantic prior basis and 3D information have



Figure 6: Ablation study for Ours, Ours (w/o basis) and Ours (w/o 3d). Ours (w/o basis) denotes our method without semantic prior basis and Ours (w/o 3d) denotes our method without 3d information.

Table 3: Experimental results on Re-score for evaluating the importance of semantic prior basis and 3d information. Best scores are highlighted in red.

Methods	Male (↓)			Young (↓)			Pose (↓)			Eyeglasses		
	FM	SG	FG	FM	SG	FG	FM	SG	FG	FM (↓)	SG (↑)	FG (↑)
Ours	0.016	0.071	0.128	0.094	0.014	0.026	0.019	0.000	0.012	0.191	0.993	0.988
w/o basis	0.096	0.132	0.228	0.204	0.051	0.072	0.019	0.015	0.038	0.015	0.992	0.974
w/o 3d	0.041	0.080	0.214	0.126	0.004	0.040	0.019	0.011	0.012	0.192	0.992	0.987

coherent synthesizing edges and intact face information, while the results without the semantic prior basis are not photo-realistic. This may be induced by the large area of the face mask compared with relatively small face images, making the network challenging to learn discrete semantic attribute representations of GAN directly. In sun glasses and frame glasses synthesis, the shape of glasses is quite blurry and aliasing without the help of semantic prior basis. In some details (such as lips and hair), the results without 3D information tend to be changed lightly. The lack of 3D information embedding makes it difficult for the network to retain the detailed information of the original image. While in our method, the synthesized images with semantic prior basis and 3D-aware embedding are more anti-aliasing and authentic.

In addition, we analyze the quantitative results of our method in terms of Re-score with and without semantic prior basis and 3d information. The detailed results are listed in Tab. 3. From Tab. 3, we observe that "Ours" apparently outperforms "Ours (w/o basis)" and "Ours (w/o 3d)" nearly on all attribute metrics. In particular, "Ours" outperforms "Ours (w/o basis)" by 0.061 on the Male attribute and outperforms "Ours (w/o basis)" by 0.015 on the pose attribute when synthesizing sun glasses. In addition, the results of "Ours (w/o basis)" are always worse in metrics. Overall, our method can coherently improve the quality of synthesized images qualitatively and quantitatively, especially when semantic prior basis is well relevant to the optimal semantic representation of the GAN model.

5 CONCLUSION

In this paper, we propose an innovative framework by decomposing semantic discrete attributes representation of GAN into semantic prior basis and offset latent representation. The semantic prior basis will be learned by the SVM classifier in the latent space of GAN and a novel semantic fusion network is proposed to generate offset latent representation of facial attributes with the guidance of face 3D information. In this way, our method can well learn accurate discrete attributes in the facial representation for synthesizing photo-realistic face images. Extensive experiments demonstrate that our method can synthesize photo-realistic face images with discrete attributes while stabilizing other attributes. In the future, we will continue to study the properties of semantics in the latent space of GANs for generic real image editing tasks.

ACKNOWLEDGMENTS

This research was supported by the National Key Research and Development Program of China (2020AAA09701), National Science Fund for Distinguished Young Scholars (62125601), National Natural Science Foundation of China (62076024, 62172035, 62006018, 61806017).

REFERENCES

- [1] Aqeel Anwar and Arijit Raychowdhury. 2020. Masked Face Recognition for Secure Authentication. *CoRR* abs/2008.11104 (2020).
- [2] Volker Blanz and Thomas Vetter. 1999. A Morphable Model for the Synthesis of 3D Faces. In *Conference on Computer Graphics and Interactive Techniques*. 187–194.

- [3] Adnane Cabani, Karim Hammoudi, Halim Benhabiles, and Mahmoud Melkemi. 2021. MaskedFace-Net - A Dataset of Correctly/Incorrectly Masked Face Images in the Context of COVID-19. *Smart Health* 19 (2021), 100144.
- [4] Eric R. Chan, Connor Z. Lin, Matthew A. Chan, Koki Nagano, Boxiao Pan, Shalini De Mello, Orazio Gallo, Leonidas Guibas, Jonathan Tremblay, Sameh Khamis, Tero Karras, and Gordon Wetzstein. 2022. Efficient Geometry-aware 3D Generative Adversarial Networks. In *IEEE Conference on Computer Vision and Pattern Recognition*.
- [5] Eric R Chan, Marco Monteiro, Petr Kellnhofer, Jiajun Wu, and Gordon Wetzstein. 2021. pi-gan: Periodic implicit generative adversarial networks for 3d-aware image synthesis. In *IEEE Conference on Computer Vision and Pattern Recognition*. 5799–5809.
- [6] Huiwen Chang, Jingwan Lu, Fisher Yu, and Adam Finkelstein. 2018. PairedCycleGAN: Asymmetric Style Transfer for Applying and Removing Makeup. In *IEEE Conference on Computer Vision and Pattern Recognition*. 40–48.
- [7] Xi Chen, Yan Duan, Rein Houthoofd, John Schulman, Ilya Sutskever, and Pieter Abbeel. 2016. InfoGAN: Interpretable Representation Learning by Information Maximizing Generative Adversarial Nets. In *Advances in Neural Information Processing Systems*. 2172–2180.
- [8] Zhiqin Chen and Hao Zhang. 2019. Learning Implicit Fields for Generative Shape Modeling. In *IEEE Conference on Computer Vision and Pattern Recognition*.
- [9] Yunjey Choi, Min-Je Choi, Munyoung Kim, Jung-Woo Ha, Sunghun Kim, and Jaegul Choo. 2018. StarGAN: Unified Generative Adversarial Networks for Multi-Domain Image-to-Image Translation. In *IEEE Conference on Computer Vision and Pattern Recognition*. 8789–8797.
- [10] Jiankang Deng, Jia Guo, Niannan Xue, and Stefanos Zafeiriou. 2019. ArcFace: Additive Angular Margin Loss for Deep Face Recognition. In *IEEE Conference on Computer Vision and Pattern Recognition*. 4690–4699.
- [11] Yu Deng, Jiaolong Yang, Jianfeng Xiang, and Xin Tong. 2022. GRAM: Generative Radiance Manifolds for 3D-Aware Image Generation. In *IEEE Conference on Computer Vision and Pattern Recognition*.
- [12] Jiatao Gu, Lingjie Liu, Peng Wang, and Christian Theobalt. 2022. StyleNeRF: A Style-based 3D Aware Generator for High-resolution Image Synthesis. In *International Conference on Learning Representations*.
- [13] Hongbin Guo, Bin Sheng, Ping Li, and C. L. Philip Chen. 2021. Multiview High Dynamic Range Image Synthesis Using Fuzzy Broad Learning System. *IEEE Transactions on Cybernetics* 51, 5 (2021), 2735–2747.
- [14] Jianzhu Guo, Xiangyu Zhu, Zhen Lei, and Stan Z. Li. 2018. Face Synthesis for Eyeglass-Robust Face Recognition. In *Biometric Recognition*. 275–284.
- [15] Jianzhu Guo, Xiangyu Zhu, Yang Yang, Fan Yang, Zhen Lei, and Stan Z. Li. 2020. Towards Fast, Accurate and Stable 3D Dense Face Alignment. In *European Computer Vision*. 152–168.
- [16] Erik Härkönen, Aaron Hertzmann, Jaakko Lehtinen, and Sylvain Paris. 2020. GANSpace: Discovering Interpretable GAN Controls. In *Advances in Neural Information Processing Systems*.
- [17] Kaiming He, Xiangyu Zhang, Shaoqing Ren, and Jian Sun. 2016. Deep Residual Learning for Image Recognition. In *IEEE Conference on Computer Vision and Pattern Recognition*. 770–778.
- [18] Yang Hong, Bo Peng, Haiyao Xiao, Ligang Liu, and Juyong Zhang. 2021. Headnerf: A real-time nerf-based parametric head model. *arXiv preprint arXiv:2112.05637* (2021).
- [19] Jie-Bo Hou, Xiaobin Zhu, Chang Liu, Chun Yang, Long-Huang Wu, Hongfa Wang, and Xu-Cheng Yin. 2020. Detecting text in scene and traffic guide panels with attention anchor mechanism. *IEEE Transactions on Intelligent Transportation Systems* 22, 11 (2020), 6890–6899.
- [20] Xueqi Hu, Qisheng Huang, Zhengyi Shi, Siyuan Li, Changxin Gao, Li Sun, and Qingli Li. 2022. Style Transformer for Image Inversion and Editing. In *IEEE Conference on Computer Vision and Pattern Recognition*.
- [21] Phillip Isola, Jun-Yan Zhu, Tinghui Zhou, and Alexei A. Efros. 2017. Image-to-Image Translation with Conditional Adversarial Networks. In *IEEE Conference on Computer Vision and Pattern Recognition*. 5967–5976.
- [22] Wentao Jiang, Si Liu, Chen Gao, Jie Cao, Ran He, Jiashi Feng, and Shuicheng Yan. 2020. PSGAN: Pose and Expression Robust Spatial-Aware GAN for Customizable Makeup Transfer. In *IEEE Conference on Computer Vision and Pattern Recognition*. 5193–5201.
- [23] Tero Karras, Miika Aittala, Samuli Laine, Erik Härkönen, Janne Hellsten, Jaakko Lehtinen, and Timo Aila. 2021. Alias-Free Generative Adversarial Networks. In *Proc. NeurIPS*.
- [24] Tero Karras, Samuli Laine, and Timo Aila. 2019. A Style-Based Generator Architecture for Generative Adversarial Networks. In *IEEE Conference on Computer Vision and Pattern Recognition*. 4401–4410.
- [25] Tero Karras, Samuli Laine, Miika Aittala, Janne Hellsten, Jaakko Lehtinen, and Timo Aila. 2020. Analyzing and Improving the Image Quality of StyleGAN. In *IEEE Conference on Computer Vision and Pattern Recognition*. 8107–8116.
- [26] Vahid Kazemi and Josephine Sullivan. 2014. One Millisecond Face Alignment with an Ensemble of Regression Trees. In *IEEE Conference on Computer Vision and Pattern Recognition*. 1867–1874.
- [27] Diederik P. Kingma and Jimmy Ba. 2015. Adam: A Method for Stochastic Optimization. In *International Conference on Learning Representations*.
- [28] Chen-Hsuan Lin, Ersin Yumer, Oliver Wang, Eli Shechtman, and Simon Lucey. 2018. ST-GAN: Spatial Transformer Generative Adversarial Networks for Image Compositing. In *IEEE Conference on Computer Vision and Pattern Recognition*. 9455–9464.
- [29] Ben Mildenhall, Pratul P Srinivasan, Matthew Tancik, Jonathan T Barron, Ravi Ramamoorthi, and Ren Ng. 2020. Nerf: Representing scenes as neural radiance fields for view synthesis. In *European conference on computer vision*. 405–421.
- [30] Ryota Natsume, Tatsuya Yatagawa, and Shigeo Morishima. 2018. RSGAN: face swapping and editing using face and hair representation in latent spaces. In *Special Interest Group on Computer Graphics and Interactive Techniques Conference*. 69:1–69:2.
- [31] Roy Or-El, Xuan Luo, Mengyi Shan, Eli Shechtman, Jeong Joon Park, and Ira Kemelmecher-Shlizerman. 2022. StyleSDF: High-Resolution 3D-Consistent Image and Geometry Generation. In *IEEE Conference on Computer Vision and Pattern Recognition*.
- [32] Fu-Zhao Ou, Xingyu Chen, Ruixin Zhang, Yuge Huang, Shaoxin Li, Jilin Li, Yong Li, Liujuan Cao, and Yuan-Gen Wang. 2021. SDD-FIQ: Unsupervised Face Image Quality Assessment with Similarity Distribution Distance. In *IEEE Conference on Computer Vision and Pattern Recognition*.
- [33] Xingang Pan, Bo Dai, Ziwei Liu, Chen Change Loy, and Ping Luo. 2021. Do 2D GANs Know 3D Shape? Unsupervised 3D Shape Reconstruction from 2D Image GANs. In *International Conference on Learning Representations*.
- [34] Jeong Joon Park, Peter Florence, Julian Straub, Richard Newcombe, and Steven Lovegrove. 2019. Deepsdf: Learning continuous signed distance functions for shape representation. In *IEEE Conference on Computer Vision and Pattern Recognition*. 165–174.
- [35] Taesung Park, Ming-Yu Liu, Ting-Chun Wang, and Jun-Yan Zhu. 2019. Semantic Image Synthesis With Spatially-Adaptive Normalization. In *IEEE Conference on Computer Vision and Pattern Recognition*. 2337–2346.
- [36] Or Patashnik, Zongze Wu, Eli Shechtman, Daniel Cohen-Or, and Dani Lischinski. 2021. StyleCLIP: Text-Driven Manipulation of StyleGAN Imagery. In *IEEE International Conference on Computer Vision*. 2085–2094.
- [37] Pascal Paysan, Reinhard Knothe, Brian Amberg, Sami Romdhani, and Thomas Vetter. 2009. A 3D Face Model for Pose and Illumination Invariant Face Recognition. In *IEEE International Conference on Advanced Video and Signal Based Surveillance*, Stefano Tubaro and Jean-Luc Dugelay (Eds.). 296–301.
- [38] Alec Radford, Jong Wook Kim, Chris Hallacy, Aditya Ramesh, Gabriel Goh, Sandhini Agarwal, Girish Sastry, Amanda Askell, Pamela Mishkin, Jack Clark, Gretchen Krueger, and Ilya Sutskever. 2021. Learning Transferable Visual Models From Natural Language Supervision. In *International Conference on Machine Learning*, Vol. 139. 8748–8763.
- [39] Joseph Redmon, Santosh Divvala, Ross Girshick, and Ali Farhadi. 2016. You only look once: Unified, real-time object detection. In *IEEE conference on computer vision and pattern recognition*. 779–788.
- [40] Oliver Richter and Roger Wattenhofer. 2018. TreeConnect: A Sparse Alternative to Fully Connected Layers. In *IEEE International Conference on Tools with Artificial Intelligence*. 924–931.
- [41] Yujun Shen, Jinjin Gu, Xiaou Tang, and Bolei Zhou. 2020. Interpreting the Latent Space of GANs for Semantic Face Editing. In *IEEE Conference on Computer Vision and Pattern Recognition*. 9240–9249.
- [42] Yujun Shen, Ceyuan Yang, Xiaou Tang, and Bolei Zhou. 2020. InterFaceGAN: Interpreting the Disentangled Face Representation Learned by GANs. *IEEE Transactions on Pattern Analysis and Machine Intelligence* (2020).
- [43] Yujun Shen and Bolei Zhou. 2021. Closed-Form Factorization of Latent Semantics in GANs. In *IEEE Conference on Computer Vision and Pattern Recognition*.
- [44] Bin Sheng, Ping Li, Chenhao Gao, and Kwan-Liu Ma. 2019. Deep Neural Representation Guided Face Sketch Synthesis. *IEEE Transactions on Visualization and Computer Graphics* 25, 12 (2019), 3216–3230.
- [45] Philipp Terhöst, Jan Niklas Kolf, Naser Damer, Florian Kirchbuchner, and Arjan Kuijper. 2020. SER-FIQ: Unsupervised Estimation of Face Image Quality Based on Stochastic Embedding Robustness. In *IEEE Conference on Computer Vision and Pattern Recognition*. 5650–5659.
- [46] Ayush Tewari, Mohamed Elgharib, Gaurav Bharaj, Florian Bernard, Hans-Peter Seidel, Patrick Pérez, Michael Zollhöfer, and Christian Theobalt. 2020. StyleRig: Rigging StyleGAN for 3D Control Over Portrait Images. In *IEEE Conference on Computer Vision and Pattern Recognition*. 6141–6150.
- [47] Ting-Chun Wang, Ming-Yu Liu, Jun-Yan Zhu, Andrew Tao, Jan Kautz, and Bryan Catanzaro. 2018. High-Resolution Image Synthesis and Semantic Manipulation With Conditional GANs. In *IEEE Conference on Computer Vision and Pattern Recognition*. 8798–8807.
- [48] Zhongyuan Wang, Guangcheng Wang, Baojin Huang, Zhangyang Xiong, Qi Hong, Hao Wu, Peng Yi, Kui Jiang, Nanxi Wang, Yingjiao Pei, Heling Chen, Yu Miao, Zhibing Huang, and Jinbi Liang. 2020. Masked Face Recognition Dataset and Application. *CoRR abs/2003.09093* (2020).
- [49] Shangzhe Wu, Christian Ruppert, and Andrea Vedaldi. 2020. Unsupervised Learning of Probably Symmetric Deformable 3D Objects From Images in the

- Wild. In *IEEE Conference on Computer Vision and Pattern Recognition*. 1–10.
- [50] Zongze Wu, Dani Lischinski, and Eli Shechtman. 2021. Stylespace analysis: Disentangled controls for stylegan image generation. In *IEEE Conference on Computer Vision and Pattern Recognition*. 12863–12872.
- [51] Ceyuan Yang, Yujun Shen, and Bolei Zhou. 2020. Semantic Hierarchy Emerges in Deep Generative Representations for Scene Synthesis. *IJCV* (2020).
- [52] Ruiyun Yu, Xiaoqi Wang, and Xiaohui Xie. 2019. VTNFP: An Image-Based Virtual Try-On Network With Body and Clothing Feature Preservation. In *IEEE International Conference on Computer Vision*. 10510–10519.
- [53] Jiaolong Yang, Yuxuan Han, and Ying Fu. 2021. Disentangled Face Attribute Editing via Instance-Aware Latent Space Search. In *International Joint Conference on Artificial Intelligence*.
- [54] Fangneng Zhan, Hongyuan Zhu, and Shijian Lu. 2019. Spatial Fusion GAN for Image Synthesis. In *IEEE Conference on Computer Vision and Pattern Recognition*. 3653–3662.
- [55] Jie Zhang, Yan Luximon, Parth Shah, Kangneng Zhou, and Ping Li. 2022. Customize My Helmet: A Novel Algorithmic Approach Based on 3D Head Prediction. *Computer-Aided Design* (2022), 1–29.
- [56] Jie Zhang, Kangneng Zhou, and Yan Luximon. 2020. A Brief Review of 3D Face Reconstruction Methods for Face-Related Product Design. In *Joint Conference of the Asian Council on Ergonomics and Design and the Southeast Asian Network of Ergonomics Societies*. 357–366.
- [57] Jie Zhang, Kangneng Zhou, Yan Luximon, Ping Li, and Hassan Iftikhar. 2022. 3D-guided facial shape clustering and analysis. *Multimedia Tools and Applications* 81, 6 (2022), 8785–8806.
- [58] Richard Zhang, Phillip Isola, Alexei A. Efros, Eli Shechtman, and Oliver Wang. 2018. The Unreasonable Effectiveness of Deep Features as a Perceptual Metric. In *IEEE Conference on Computer Vision and Pattern Recognition*. 586–595.
- [59] Shi-Xue Zhang, Xiaobin Zhu, Lei Chen, Jie-Bo Hou, and Xu-Cheng Yin. 2022. Arbitrary Shape Text Detection via Segmentation with Probability Maps. *IEEE Transactions on Pattern Analysis and Machine Intelligence* (2022).
- [60] Shi-Xue Zhang, Xiaobin Zhu, Jie-Bo Hou, Chun Yang, and Xu-Cheng Yin. 2022. Kernel Proposal Network for Arbitrary Shape Text Detection. *IEEE Transactions on Neural Networks and Learning Systems* (2022).
- [61] Shi-Xue Zhang, Xiaobin Zhu, Chun Yang, Hongfa Wang, and Xu-Cheng Yin. 2021. Adaptive boundary proposal network for arbitrary shape text detection. In *Proceedings of the IEEE/CVF International Conference on Computer Vision*. 1305–1314.
- [62] Xuanmeng Zhang, Zhedong Zheng, Daiheng Gao, Bang Zhang, Pan Pan, and Yi Yang. 2022. Multi-View Consistent Generative Adversarial Networks for 3D-aware Image Synthesis. In *CVPR*.
- [63] Peng Zhou, Lingxi Xie, Bingbing Ni, and Qi Tian. 2021. Cips-3d: A 3d-aware generator of gans based on conditionally-independent pixel synthesis. *arXiv preprint arXiv:2110.09788* (2021).
- [64] Jun-Yan Zhu, Taesung Park, Phillip Isola, and Alexei A. Efros. 2017. Unpaired Image-to-Image Translation Using Cycle-Consistent Adversarial Networks. In *IEEE International Conference on Computer Vision*. 2242–2251.
- [65] Jiapeng Zhu, Yujun Shen, Deli Zhao, and Bolei Zhou. 2020. In-Domain GAN Inversion for Real Image Editing. In *European Conference Computer Vision*. 592–608.
- [66] Peihao Zhu, Rameen Abdal, Yipeng Qin, and Peter Wonka. 2020. SEAN: Image Synthesis With Semantic Region-Adaptive Normalization. In *IEEE Conference on Computer Vision and Pattern Recognition*. 5103–5112.
- [67] Xiaobin Zhu, Zhuangzi Li, Jungang Lou, and Qing Shen. 2021. Video super-resolution based on a spatio-temporal matching network. *Pattern Recognition* 110 (2021), 107619.
- [68] Xiaobin Zhu, Zhuangzi Li, Xiao-Yu Zhang, Changsheng Li, Yaqi Liu, and Ziyu Xue. 2019. Residual invertible spatio-temporal network for video super-resolution. In *Proceedings of the AAAI conference on artificial intelligence*, Vol. 33. 5981–5988.
- [69] Xiangyu Zhu, Xiaoming Liu, Zhen Lei, and Stan Z Li. 2017. Face alignment in full pose range: A 3d total solution. *IEEE transactions on pattern analysis and machine intelligence* (2017).

A OVERVIEW

This supplementary material contains the following parts:

- We introduce the architecture details of style encoder and fusion modules of the proposed 3D-aware semantic fusion network.
- We provide extra experiments to prove the performance of our method.
- We provide some example images in our proposed MEGN (Face Mask and Eyeglasses images crawled from Google and Naver).

- We propose a video to show discrete attribute manipulation results (see MM.mp4 in the supplement zip).

B ARCHITECTURE DETAILS

Following the networks in SPADE [35] and SEAN [66], we design the structure of style encoder and fusion module to synthesize face with discrete attributes.

B.1 Style Encoder

As shown in Fig. 7 (a), our style encoder consists of multi-layer convolutions to extract 3D features from the concatenation of face normal map, diffuse map, and albedo images. The region-wise average pooling is adopted here to get style feature. The pooling mainly aims to adapt the dimensions of the subsequent module.

B.2 Fusion Module

As shown in Fig. 7 (b), our fusion module adopts weighted learning with coefficients to fuse the extracted features. Specifically, the style feature undergoes a per-style convolution and is then broadcast to face feature. In this way, the style map is yielded. The style map is processed by convolution layers to produce pixel normalization values of 3D information. The face feature passes through a convolution layer and then two separate convolution layers to obtain pixel normalization values of face. The learnable weight parameters α_1 and α_2 during training would adjust the proportion of each variable when fusing with attribute feature.

C EXTRA EXPERIMENTS

C.1 Image Quality Estimation

In our experiments, we adopt SDD-FIQA [32] and SER-FIQ [45] to evaluate the realism of synthesized images. SDD-FIQA [32] and SER-FIQ [45] are two popular metrics in evaluating the effectiveness of image data for the face recognition task. The higher scores of SDD-FIQA and SER-FIQ denote the better quality of synthesized images. The detailed results are listed in Tab. 4.

From Tab. 4, we observe that our method outperforms other methods in terms of SDD-FIQA and SER-FIQ in face mask synthesis. Notably, our method outperforms InterfaceGAN [41] in face mask synthesis by 5.95 in terms of SDD-FIQA. Although InterfaceGAN achieves a higher SDD-FIQA score (68.652) than Ours (56.350) on sum glasses synthesis, it significantly modifies other attributes, as shown in Fig. 9,10,11. And this is detrimental for many tasks, such as data augmentation for face recognition. Overall, our method achieves promising quality for face image synthesis and can significantly benefit data augmentation in face recognition-related tasks.

C.2 Decoupled Degree Between Attributes

In this section, we study the decoupled degrees between attributes to reflect if attribute subspace is correctly divided in latent space. Here, we use cosine similarity to measure the decoupled degree between two semantic representations. A large value of cosine similarity indicates a bad decoupled degree of two attributes. We compare our method with InterfaceGAN [41]. The detailed results are shown in Fig. 8. The attributes (age, beauty, light, gender, face

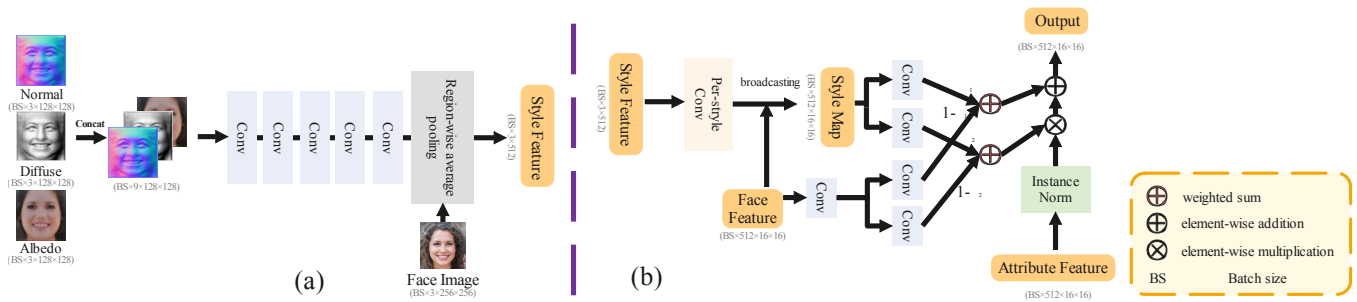


Figure 7: The architecture of style encoder and fusion module.

Table 4: Experimental results of face image quality estimation with SDD-FIQA and SER-FIQ. The best SDD-FIQA and SER-FIQ are highlighted in red, and the second-best results are highlighted in blue. FM denotes face mask, SG denotes sun glasses and FG denotes frame glasses.

Methods	SDD-FIQA [32] (\uparrow)			SER-FIQ [45] (\uparrow)		
	FM	SG	FG	FM	SG	FG
Ground-truth	58.017	55.854	66.045	0.874	0.767	0.885
ST-GAN [28]	/	53.329	65.691	/	0.816	0.875
Pix2Pix[21]	56.102	50.326	63.319	0.880	0.491	0.879
CycleGAN[64]	58.222	55.482	66.272	0.878	0.775	0.883
InterfaceGAN [41]	55.523	68.652	68.507	0.877	0.889	0.889
StyleCLIP [36]	55.720	54.694	55.574	0.880	0.886	0.885
Ours	61.473	56.350	64.789	0.881	0.859	0.884

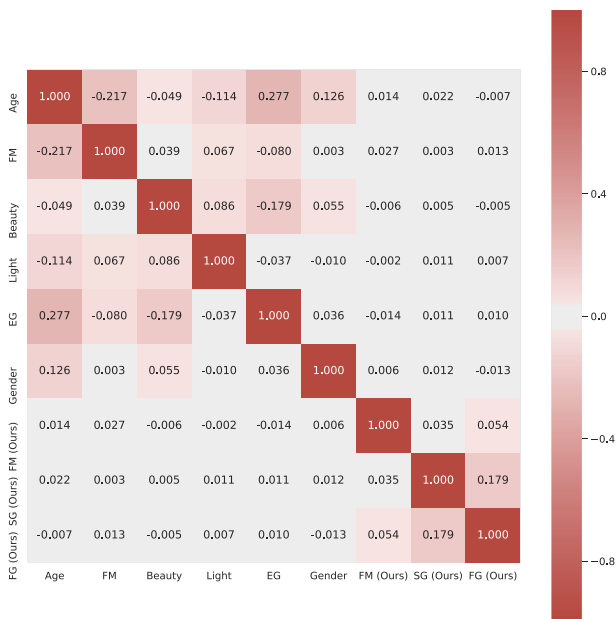


Figure 8: Experimental results of decoupled relationships between attributes. A large value of cosine similarity indicates a bad decoupled degree of two attributes. Our method outperforms InterfaceGAN with a significant margin.

mask, and glasses) obtained by InterfaceGAN [41] have a bad decoupled relation between each other. Especially, the decoupled degree between age and face mask reaches 0.217, the decoupled degree between age and glasses reaches 0.277, the decoupled degree between beauty and glasses reaches 0.179. In our method, the decoupled degrees between attributes are all approximate to 0. This indicates that attribute representations in our method are almost orthogonal with each other. In particular, our method uncouples age with glasses, age with face mask, and beauty with sun glasses, resulting in superior decoupled degree 0.007, 0.014, and 0.005, respectively. Apparently, our method outperforms InterfaceGAN [41] in the capability of decoupling relationships between different attributes with a significant margin.

C.3 Additional Results

We provide additional results to those presented in the paper. In Fig. 9,10,11, we show a large number of visual results of face mask, frame glasses and sun glasses synthesis methods separately. Our method keeps other face attributes intact and also synthesizes face images with visual details especially on anti-aliasing.

D OUR PROPOSED MEGN

We propose a big dataset MEGN (Face Mask and Eyeglasses images crawled from Google and Naver) which includes 5,000 face images with discrete attributes. See Fig. 12 for some representative images. Existing face image datasets with discrete attributes only have small and fuzzy images. To the best of our knowledge, our MEGN is the

first realistic, high-definition dataset of face images with discrete attributes, especially face mask.



Figure 9: Representative visual results of discrete face mask attribute synthesis. Other methods have poor performance on discrete face mask and fail retain face attributes while editing. Our method outperforms other methods on visual quality especially anti-aliasing and other face attributes intactness.

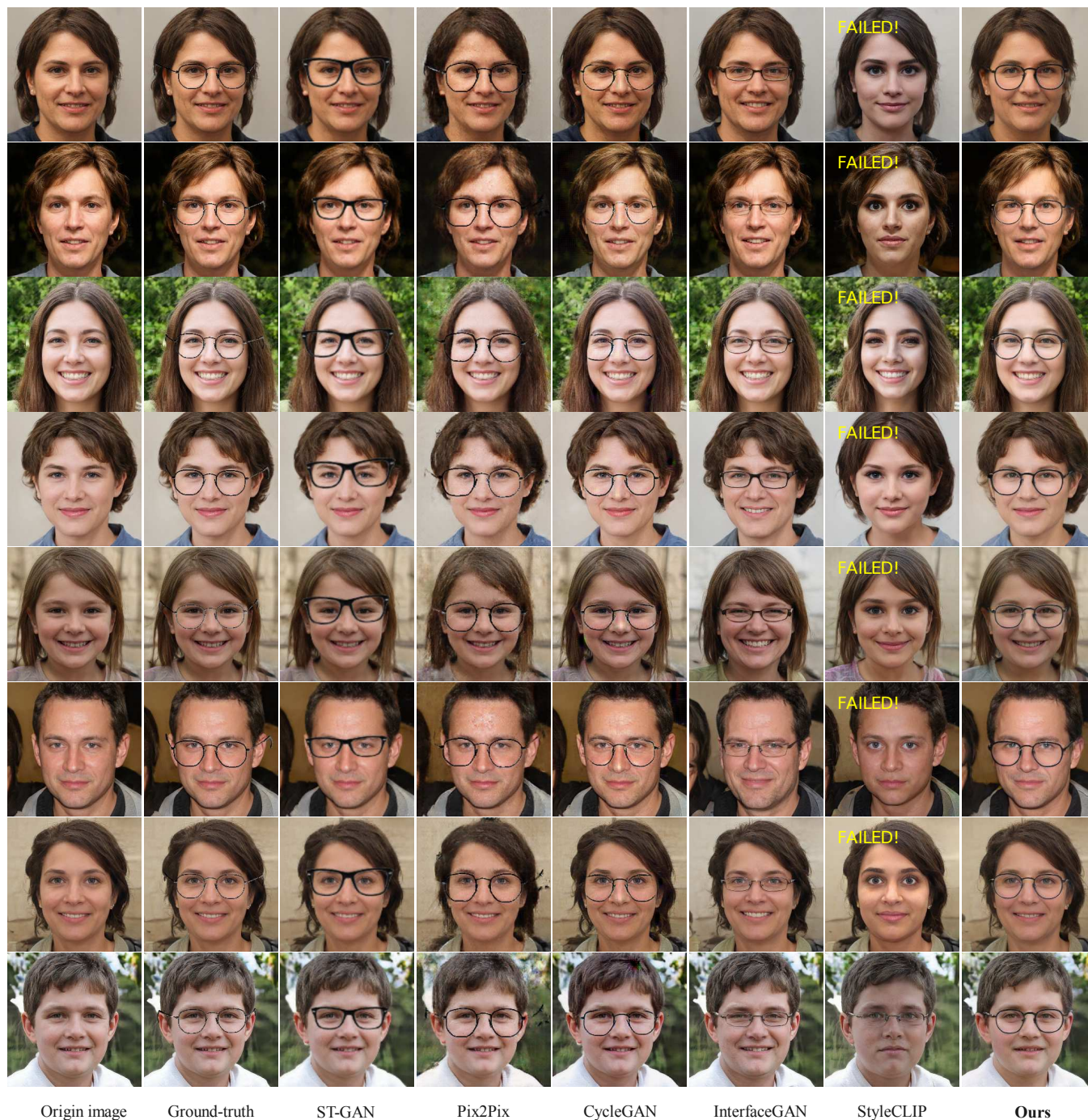


Figure 10: Representative visual results of discrete frame glasses attribute synthesis. Other methods have poor performance on discrete frame glasses and fail retain face attributes while editing. Our method outperforms other methods on visual quality especially anti-aliasing and other face attributes intactness.

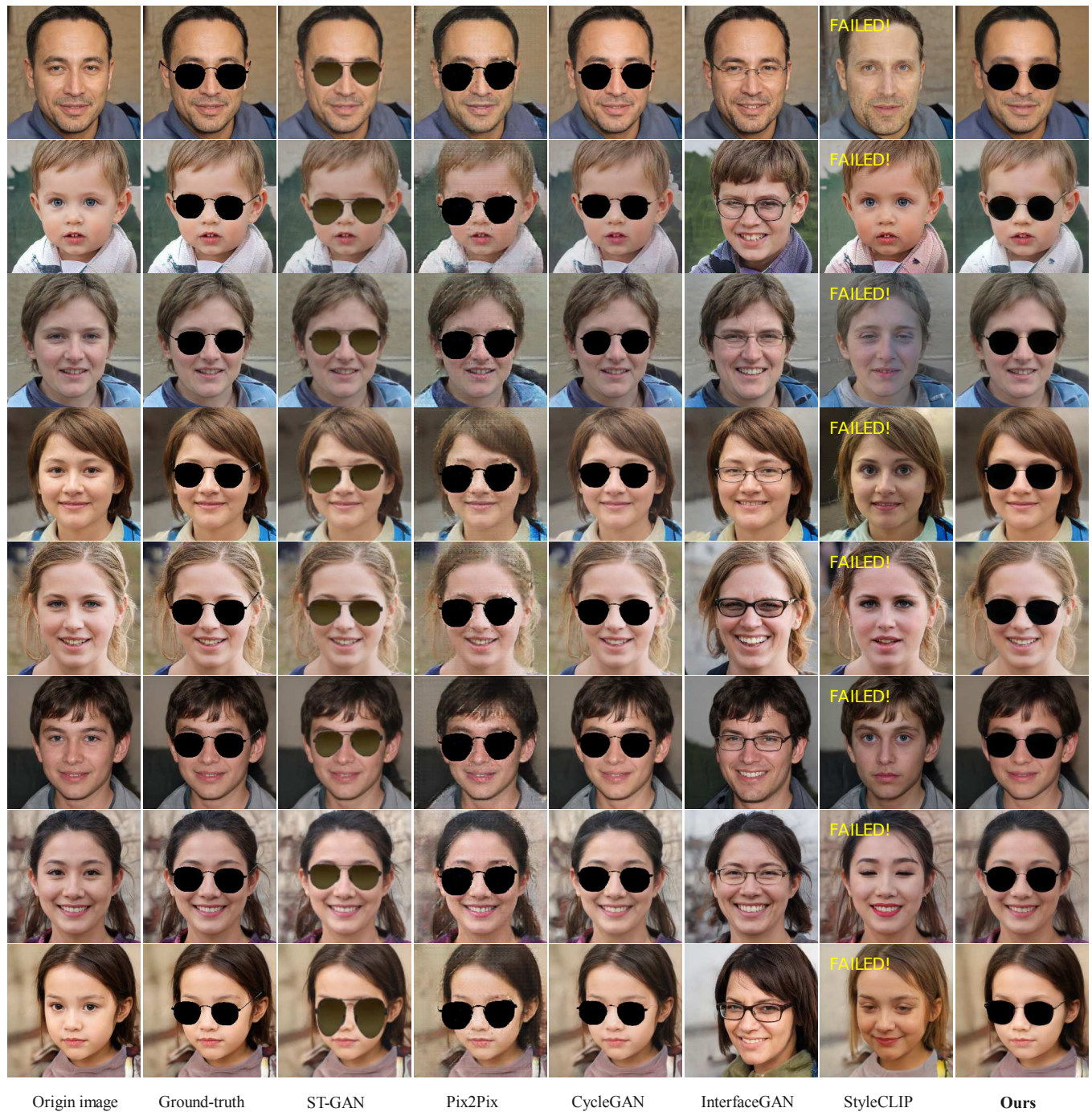


Figure 11: Representative visual results of discrete sun glasses attribute synthesis. Other methods have poor performance on discrete sun glasses and fail retain face attributes while editing. Our method outperforms other methods on visual quality especially anti-aliasing and other face attributes intactness.



Figure 12: Some example images in MEGN. Our MEGN is the first realistic, high-definition dataset of face images with discrete attributes, especially face mask.